J. Fluid Mech. (2011), *vol.* 669, *pp.* 214–224. © Cambridge University Press 2011
doi:10.1017/S0022112010006154

Hollow wakes past arbitrarily shaped obstacles

H. TELIB AND L. ZANNETTI†

DIASP, Politecnico di Torino, Corso Duca degli Abruzzi 24, 10129 Turin, Italy

(Received 6 October 2010; revised 24 November 2010; accepted 26 November 2010;
first published online 1 February 2011)

An analytical solution is presented for steady inviscid separated flows modelled by hollow vortices, that is, by closed vortex sheets bounding a region with fluid at rest. Steady flows past arbitrary obstacles protruding from an infinite wall are considered. The solution is similar to that of the vortex patch model; it depends on two free parameters that define the size of the hollow vortex and the location of the separation point. When a sharp edge constrains the separation point (Kutta condition), the solution depends on a single parameter. As with the vortex patch model, families of growing vortices exist, which represent the continuation of desingularized point vortices. Numerical results are presented for the flows past a semicircular bump, a Ringleb snow cornice and a normal flat plate. The differences from the previous results found in the literature are analysed and discussed with the present solutions for the flow past a normal flat plate.

Key words: separated flows, vortex dynamics, wakes

1. Introduction

The paper concerns inviscid steady two-dimensional flows which separate from arbitrarily shaped obstacles protruding from an infinite wall. For given far-field boundary conditions, if the wake has a finite area, multiple solutions exist. They correspond to different vorticity distributions $\xi(\psi)$ along the closed streamlines that form the wake.

Among these multiple solutions, Batchelor (1956) showed that the limit of the viscous wake for the Reynolds number tending to infinity is a '$\xi =$ constant' vortex patch bounded by a mixing/boundary layer with vanishing thickness, that is, by a vortex sheet. This flow is called the Prandtl–Batchelor (P–B) flow. It consists of a potential flow whose streamlines extend to infinity and of a wake formed by a vortex patch bounded by a vortex sheet.

As discussed by Chernyshenko (1998) and Gallizio *et al.* (2010) and the references therein, the values of the vorticity and of the jump of the Bernoulli constant across the vortex sheet are defined by the condition that the boundary layer/mixing layer is cyclic and by the location of the separation point. Thus, if the obstacle presents a sharp edge which fixes the separation point (Kutta condition), the P–B flow is fully defined.

† Email address for correspondence: luca.zannetti@polito.it

https://doi.org/10.1017/S0022112010006154 Published online by Cambridge University Press

Let a vortex patch, bounded by a vortex sheet and surrounded by a cyclic potential flow, be assumed as the inviscid wake model. The resulting flow is governed by the equation

$$\nabla^2\psi = -\xi\, H(\alpha - \psi) + \beta\, \delta(\alpha - \psi), \tag{1.1}$$

where H and δ are the Heaviside and Dirac functions; α is the value of the stream function on the patch boundary; and β is the jump of the Bernoulli constant across the vortex sheet. For given far-field boundary conditions, the solutions of (1.1) form a family in the three-dimensional (ξ, α, β) parameter space. In an equivalent way, (γ, D, β) can be assumed to be parameters, where γ is the wake circulation and D is the patch area.

For $\alpha = \psi_o$, with ψ_o denoting the value of the stream function at the solid boundary, the wake family includes the P–B flow solution. At the other extremum, for $D \to 0$ ($|\alpha| \to \infty$) and $|\xi| \to \infty$, the model includes the solution represented by a point vortex standing in equilibrium. Elcrat *et al.* (2000) provided examples of such a family of wakes for the flow past a semicircular bump. They restricted the analysis to $\beta = 0$ and showed that, for values of γ relevant to point vortices standing on the Föppl curve, the entire family exists from the point vortex to the vortex patch that fills the wake.

Gallizio *et al.* (2010) addressed the implications of the Kutta condition when the location of the separation is constrained by a sharp edge. Again for $\beta = 0$, they showed that the Kutta condition implies a relationship $\gamma = \gamma(D)$ and that a given solution can be continued by varying D. This result attributes a great significance to the point vortex solutions ($D = 0$) which satisfy the Kutta condition. In fact, it can be conjectured that if a vortex patch which satisfies the Kutta condition can be continued up to the point vortex solution, bodies which do not permit point vortex solutions should not permit solutions with finite-area vortex patches either. As explained in Gallizio *et al.* (2010) and the references therein, this aspect is relevant for the problem of controlling wakes.

As proved by Smith & Clark (1986), a normal flat plate is an example of a body that does not have a point vortex which satisfies the Kutta condition. This issue was addressed for arbitrarily shaped obstacles in Zannetti (2006). Numerical results, like those obtained by Turfus (1993) for finite-area wakes past normal flat plates, seem to contradict the above conjecture; however, as discussed by Gallizio (2004) and Gallizio *et al.* (2010), the contradiction could be due to poor numerical convergence.

In the present work, the parameter space, in which solutions to (1.1) are sought, is reduced to two dimensions (β, α) by assuming $\xi = 0$. Since the wake is assumed to have a finite area, the streamline $\psi_c = \alpha$, which bounds the core, is closed, and as a consequence of $\xi = 0$, the solution inside the core is $\psi = \psi_c = \text{constant}$; that is, the wake is hollow, with the core formed by a body of fluid at rest, bounded by a vortex sheet which has the constant velocity $q_c = \sqrt{2\beta}$ on its outer side. The advantage of such a model is that the solution can be obtained almost analytically by exploiting the classical techniques of conformal mapping and hodograph-plane methods.

Hollow vortices were studied in the 19th century, for instance, by Hicks (1883) and Pocklington (1895) (see also Tanveer 1984, 1986). Classical solutions were obtained for the case of open wakes by Kirchhoff (see Lamb 1932) for a normal flat plate and by Levi-Civita (1907) for arbitrarily shaped bodies.

The typical features of a hollow wake are shown in figure 1, which shows a solution for the flow past a semicircular bump. The flow separates at A and reattaches at B.

https://doi.org/10.1017/S0022112010006154 Published online by Cambridge University Press

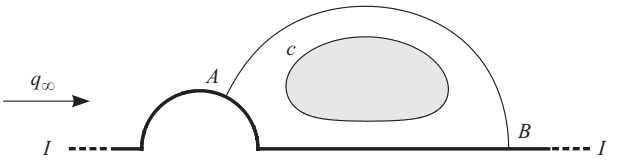


FIGURE 1. The flow pattern in the physical z-plane ($\gamma = -16.61,\ R = 0.5$).

The wake is formed by a stagnating core bounded by the c-curve and is furthermore formed by the cyclic potential flow entrained between the separatrix A–B, the solid wall and the c-curve.

The family of solutions on the (β, α) parameter space is similar to that of the vortex patch model of Elcrat *et al.* (2000); that is, for $|\alpha| \to \infty$ the solution tends towards the point vortex solution. It is more complicated to predict the limit for $\alpha \to \psi_o$. In fact, when α approaches the wall value ψ_o, the potential layer shrinks, with the core coming closer and closer to the wall. However, for $\alpha = \psi_o$ the vortex sheet detaches from the wall; the wake is of the kind studied by Levi-Civita (1907), and depending on the separation location, it will or will not reattach downstream, with the separation and possible reattachment changing from being orthogonal to being tangent to the wall. More details on this matter can be found in Birkoff & Zarantonello (1957), Gilbarg (1960) and Gurevich (1965). Moreover, as long as the hollow does not touch the wall ($\alpha \neq \psi_o$), the flow depends on the shape of the entire wall, while when the vortex sheet detaches from the wall ($\alpha = \psi_o$), the flow no longer depends on the shape of the wall segment included between the separation and possible reattachment. This implies that, in general, different walls, which admit different hollow wakes, can admit the same Levi-Civita wake. This issue concerning the limiting behaviour of hollow vortices is here left unanswered, as it is sufficient for the present study to consider the hollow-wake model as another way of desingularizing and continuing the point vortex solution.

When the Kutta condition has to be satisfied, a relationship $\alpha = \alpha(\beta)$ is set, and the flow depends on a single parameter. As previously stated, a conjecture can be made about the relationship between the existence of point vortex solutions and the desingularized solutions obtained by varying the free parameter.

The same wake model was studied by Lin & Landweber (1977), who attributed the original idea to Lavrentiev (1962). Lin & Landweber (1977) presented a method for the solution of the wake past an isolated bluff body under the assumption that the body is symmetric with respect to the far-field flow direction. Their method was formulated for arbitrary symmetric bodies, but in fact, it is applicable only for bodies with straight walls, such as normal plates or symmetric wedges, which are the only applications they described.

The solutions presented for a normal flat plate are intriguing. In fact, their method implicitly satisfies the Kutta condition, but a normal flat plate does not permit a point vortex in equilibrium that satisfies the Kutta condition, and according to the above conjecture, desingularized solutions should not exist either.

The motivation behind the present study is to provide a method that is capable of computing hollow wakes in the flow past a larger class of arbitrary bodies, which includes the symmetric bodies studied by Lin & Landweber (1977) as a subclass. Examples are presented for various geometries and flow parameters. A comparison is presented with the results of Lin & Landweber (1977), which may clarify the above

https://doi.org/10.1017/S0022112010006154 Published online by Cambridge University Press

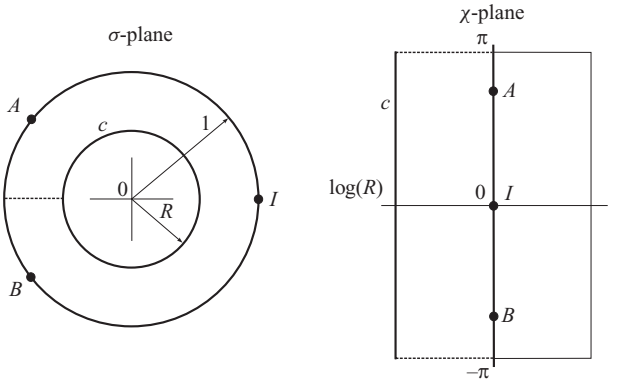


FIGURE 2. Transformed σ and χ planes.

contradiction and strengthens the conjecture about the relationship between point vortices and their desingularizations.

2. The mathematical formulation

Let figure 1 be considered as a general example of the flow field. As a consequence of the Riemann mapping theorem, a conformal transformation $z = f(\sigma)$ exists which maps the doubly connected domain of the physical complex z-plane, bounded by the solid wall and by the boundary c of the hollow, onto a circular ring of the transformed σ-plane, which, as shown in figure 2, is formed by the unit circle and by an inner circle whose radius is R.

The solution of the inverse problem of finding the geometry of the hollow is solved here by determining the mapping $z = f(\sigma)$ so that the velocity on the boundary of the hollow is constant.

As shown in figure 2, the further transformation $\chi = \log\sigma$ maps the ring onto a rectangle of the χ-plane. As described hereafter, the complex potential of the motion w can be determined as a function of χ. From $\mathrm{d}w/\mathrm{d}z = (\mathrm{d}w/\mathrm{d}\chi)(\mathrm{d}\chi/\mathrm{d}z)$, the condition that the velocity on the c-curve has to hold the constant q_c value yields

$$\left|\frac{\mathrm{d}f}{\mathrm{d}\sigma}\right|_c = \left(\frac{|\mathrm{d}w/\mathrm{d}\chi|}{R\,q_c}\right)_c, \tag{2.1}$$

which is the equation that is exploited to find the function $z = f(\sigma)$. The solution is thus obtained by mapping back ($\sigma \to z$) the circular ring of the σ-plane onto the physical z-plane.

2.1. *The complex potential w on the χ-plane*

The rectangle of the χ-plane ($\log R \leqslant \mathrm{Re}(\chi) \leqslant 0$, $-\pi \leqslant \mathrm{Im}(\chi) < \pi$), shown in figure 2, is the χ-image of the flow field bounded by the wall and by the hollow. The vertical sides correspond to the bounding streamlines; the horizontal sides represent a periodic boundary; and the origin I corresponds to the physical infinity.

As a consequence of the geometrical periodicity and of the infinite reflections needed to assure that the vertical sides are streamlines, the complex velocity $\mathrm{d}w/\mathrm{d}\chi$ is a doubly periodic function that possesses the half-periods $\omega = -\log R$ and $\omega' = \mathrm{i}\pi$. The pertinent periodic domain is drawn in figure 2. Moreover, the complex velocity $\mathrm{d}w/\mathrm{d}\chi$ has a second-order pole for $\chi = 0$ which represents the far-field flow on the

https://doi.org/10.1017/S0022112010006154 Published online by Cambridge University Press

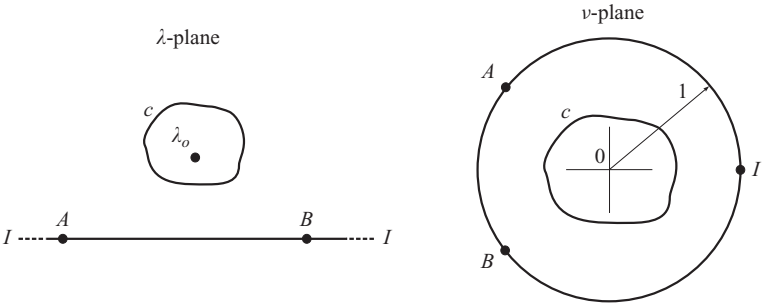


FIGURE 3. Transformed λ and ν planes.

physical plane; thus, it is expressed by an elliptic function whose general form is

$$\frac{\mathrm{d}w}{\mathrm{d}\chi} = \mathrm{i}\,Q[\wp(\chi;\omega,\omega') + \kappa], \tag{2.2}$$

where $\wp$ is the Weierstrass $\wp$-function and Q and κ are real constants. For the sake of brevity, the dependence of the elliptic functions on their half-periods (ω,ω') is omitted in what follows.

The value of κ is defined by the values of the zeros (χ_A,χ_B) of $\mathrm{d}w/\mathrm{d}\chi$. According to the properties of the poles and zeros of the elliptic functions, $\chi_B = -\chi_A$ (see, for instance, Tricomi 1951). Since $\wp$ is an even function, $\kappa = -\wp(\chi_A) = -\wp(\chi_B)$. The value of Q is related to the q_∞ value of the flow velocity at infinity by

$$Q = -\mathrm{i}\,q_\infty \lim_{\chi\to 0} \frac{\mathrm{d}z/\mathrm{d}\chi}{\wp(\chi)-\kappa}. \tag{2.3}$$

By integrating (2.2), the complex potential becomes

$$w = \mathrm{i}\,Q[-\zeta(\chi) + \kappa\,\chi] + \text{constant},$$

where ζ is the Weierstrass ζ-function. The wake circulation is $\gamma = w(-\omega + 2\omega') - w(-\omega)$; that is, according to the semi-periodicity of the ζ-function,

$$\gamma = 2\mathrm{i}\,Q\,(-\eta' + \mathrm{i}\kappa\,\pi), \tag{2.4}$$

with $\eta' = \zeta(\omega')$.

2.2. *The mapping*

The mapping $z = f(\sigma)$ is thought of as a chain of mappings. First, the simply connected flow domain is mapped onto the upper half of the λ-plane (figure 3) by means of a standard mapping, with the solid wall mapped onto the real axis, the infinity mapped onto the infinity and $(\mathrm{d}z/\mathrm{d}\lambda)_\infty = 1$. For instance, for the circular bump in figure 1, this mapping is the Joukowski transformation.

The upper λ-plane is mapped inside the unit circle of the ν-plane by the Möbius transformation $\nu = (\lambda-\lambda_o)/(\lambda-\lambda_o^\star)$, where * denotes conjugate and λ_o is guessed as a point inside the as-yet-unknown λ-image of boundary c of the hollow. The mapping is such that $\lambda = \lambda_o$ is mapped onto $\nu = 0$ and $\lambda = \infty$ onto $\nu = 1$.

The Garrick transformation, in the form proposed by Ives (1976),

$$\nu = \sigma \exp\left\{\mathrm{i}\,b_0 + \sum_{n=1}^{N}[(-a_n + \mathrm{i}\,b_n)(R\,\sigma)^n + (a_n + \mathrm{i}\,b_n)(R/\sigma)^n]\right\}, \tag{2.5}$$

https://doi.org/10.1017/S0022112010006154 Published online by Cambridge University Press

maps the circular ring of the σ-plane (figure 2) onto the doubly connected domain of the ν-plane bounded by the unit circle and by the ν-image of the c-curve (figure 3). By setting $b_0 = -2\sum_{n=1}^{N} b_n R^n$, the $\sigma = 1$ point corresponds to $\nu = 1$; that is, it corresponds to the the physical infinity.

The solution is obtained by determining the coefficients of the series, which is truncated at a suitably large value N. A numerical procedure that exploits (2.1) is used for this purpose.

According to (2.3), the value of the parameter Q is

$$Q = 2\frac{q_\infty \mathrm{Im}(\lambda_o)}{(\mathrm{d}\nu/\mathrm{d}\sigma)_{\sigma=1}}. \tag{2.6}$$

2.3. *The parameter space*

As mentioned in § 1, the governing equation (1.1) for $\xi = 0$ depends on two free parameters, namely the jump of the Bernoulli constant β and the value α of the stream function at the boundary of the hollow. For a given far-field boundary condition, that is, for a given q_∞ and for a given solid wall geometry, the solutions take place in a two-dimensional parameter manifold. For the present method, it is more convenient to select the radius R of the inner circle of the ring on the σ-plane and the value of the χ_A image of the separation point as equivalent free parameters. If a Kutta condition has to be satisfied, a relationship $\chi_A(R)$ exists, and the choice of the free parameters reduces to choose the value of R.

3. The numerical procedure

The problem is solved by determining the a_n, b_n $(n = 1, \ldots, N)$ values of the series coefficients in (2.5) and the value of the velocity q_c on the boundary c of the wake core.

The problem is similar to the pertinent direct problem, that is, to the determination of the Garrick mapping $\nu(\sigma)$ (2.5) for a known shape of the c-curve on the ν-plane. In Ives (1976), the direct problem was solved by enforcing (2.5) in $2N$ collocation points, which allows the computation of the value of R and of $2N-1$ values of (a_j, b_j). The problem was closed by setting $b_N = 0$. In a similar way, the present inverse problem is solved by enforcing (2.1), recast in the form

$$q_c - \left| \frac{\mathrm{d}w/\mathrm{d}\chi}{R\,(\mathrm{d}\nu/\mathrm{d}\sigma)(\mathrm{d}z/\mathrm{d}\nu)} \right|_c = 0, \tag{3.1}$$

for $2N$ values of σ on the circle with radius R and by computing the value of q_c and the $2N-1$ values of the coefficients a_n and b_n. The problem, as for the direct case, is closed by setting $b_N = 0$.

An under-relaxed Newton method is employed to find the root of (3.1). The Jacobian is found numerically via first-order one-sided finite differences. The resulting linear system is solved exactly by using a lower–upper (or LU) factorization. Under-relaxation is needed, especially during the first iterations, in order to obtain a robust scheme. The number of degrees of freedom is $2N = 196$ in the examples reported in § 4. This resolution has been chosen empirically in order to assure non-oscillatory behaviour of the solution. The nonlinear residual tolerance, measured as the maximum defect of (3.1) in all the collocation points, is set at 10^{-9}.

As elucidated by Nehari (1975), the mapping of a given doubly connected domain onto a circular ring is unique, with a unique value of the radius ratio R, and the

https://doi.org/10.1017/S0022112010006154 Published online by Cambridge University Press

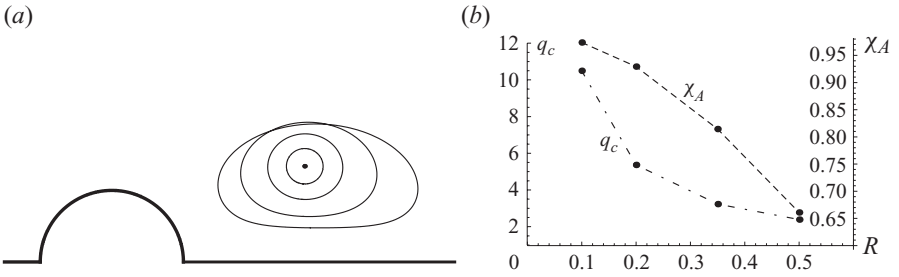


FIGURE 4. (*a*) Point vortex and growing hollows for $\gamma = -16.61$. (*b*) Parameter space path.

arbitrary choice of the parameter λ_o therefore does not affect the $z = f(\sigma)$ mapping. Different choices of λ_o imply different values of the series coefficients in (2.5), which result in the function $z = f(\sigma)$ remaining unchanged. The choice of λ_o is important with respect to the convergence of the iterative process. In fact, the Garrick mapping requires that the ν-image of the hollow is star shaped, but as R increases, the resulting ν-image is farther from a circle. In practice, a good choice is to select λ_0 so that the centroid of the c-curve maps close to the origin on the ν-plane.

The computation is initialized by considering the point vortex solution (see Zannetti 2006) pertinent to the χ_A selection. A close-to-the-point-vortex streamline is selected and is assumed as the initial guess of the c-curve pertinent to a small value of R. The initial set of (a_n, b_n) values is obtained by solving the above-outlined direct Garrick analysis. In this way, a first solution is computed for an initially small value of R. Further solutions are obtained for larger values by continuation, that is, by using the previous solutions as initial guesses.

When the Kutta condition is imposed, the physical separation point z_A is fixed, and the free parameter choice reduces to the selection of the value of R. A value of χ_{Ak} is computed at each Newton kth iteration, by numerically solving the implicit equation $z_A = f_k(\mathrm{e}^{\chi_{Ak}})$.

4. Numerical examples

Examples of hollow wakes are here shown for flows past a semicircular obstacle, a Ringleb snow cornice (see Ringleb 1961) and a normal flat plate. The flow properties are normalized by assuming the asymptotic velocity q_∞ as the reference velocity and the obstacle height as the reference length.

4.1. *Wake past a semicircular obstacle*

The present method has been used to desingularize the Föppl point vortex with $\gamma = 16.61$. As shown in figure 4, hollow wakes, with the same circulation as the point vortex, have been computed for $R = 0.10$, 0.20, 0.35 and 0.50. In order to attain the prescribed value of γ, the pertinent values of χ_A have been determined, during the iteration process, by combining (2.4) and (2.6). The computed growing hollows are shown in figure 4(*a*), and the corresponding parameter-space path is shown in figure 4(*b*). The separation points are located on the circle at the angles $\vartheta_A = 66.91°$, 66.81°, 65.95° and 63.53°, respectively. Figure 1 shows the shape of the entire wake for $R = 0.5$.

https://doi.org/10.1017/S0022112010006154 Published online by Cambridge University Press

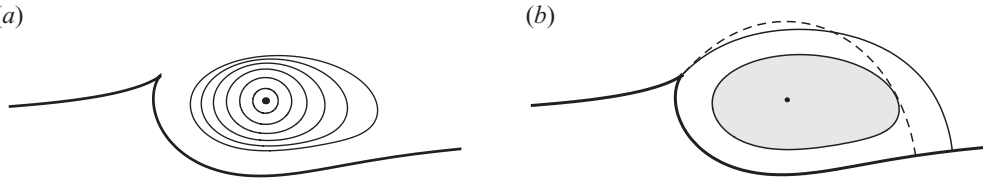


FIGURE 5. (*a*) Point vortex and growing hollows for a Ringleb snow cornice. (*b*) Point vortex and $R = 0.6$ separatrices.

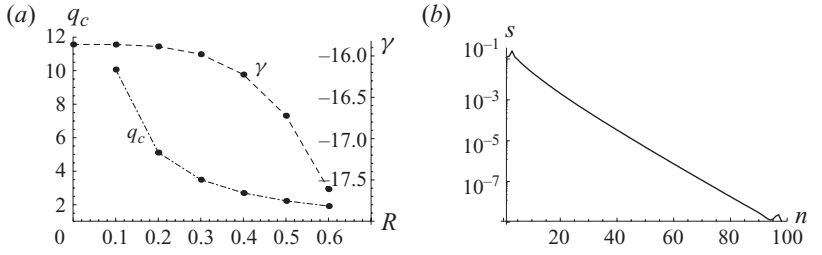


FIGURE 6. Plots of (*a*) q_c and γ versus R and (*b*) $s = \sqrt{a_n^2 + b_n^2}$ versus n for $R = 0.60$.

4.2. *Wake past a Ringleb snow cornice*

The Ringleb snow cornice, defined by the $z = \lambda + \lambda_1^2/(\lambda - \lambda_1)$ mapping (see Ringleb 1961), has been considered for $\lambda_1 = 1 - \mathrm{i}$. It is cusped in $z(0)$, and as a consequence, the flow past it has to satisfy the Kutta condition.

Wakes have been computed for the point vortex solution (see Zannetti 2006) and for hollows defined by $R = 0.10$, 0.20, 0.30, 0.40, 0.50 and 0.60. The point vortex and the shapes of the hollows are shown in figure 5(*a*). The separatrix pertinent to the point vortex (dotted line) is compared with the separatrix pertinent to $R = 0.6$ in figure 5(*b*).

Figure 6(*a*) shows the path followed by the solutions in the (R, q_c) and (R, γ) parameter spaces, which are equivalent to the original (R, χ_A) space. The aliasing of the velocity distribution along the boundary of the hollow is negligible, as can be inferred from figure 6(*b*), where, for the most unfavourable $R = 0.60$ case, the quantity $s = \sqrt{a_n^2 + b_n^2}$ is plotted versus n, showing how the series coefficients of (2.5) decay as the index n increases.

4.3. *Wake past a normal flat plate*

Lin & Landweber (1977) presented the solutions of hollow wakes past a normal flat plate. Briefly, by translating their notations in terms of the notations adopted here, their method is based on determining the $\mathrm{d}z/\mathrm{d}\chi$ mapping derivative expressed by $\mathrm{d}z/\mathrm{d}\chi = (\mathrm{d}w/\mathrm{d}\chi)/(\mathrm{d}w/\mathrm{d}z)$. The term $\mathrm{d}w/\mathrm{d}\chi$ is the same as the present one, and $\mathrm{d}w/\mathrm{d}z$ is elegantly inferred as a function of χ by considering its periodicity, zeros and singularities. The derivative $\mathrm{d}z/\mathrm{d}\chi$ depends on five parameters that have to satisfy four implicit equations. Thus a parameter can be freely chosen, and the other four are derived by numerically solving a set of four equations. Since the method is such that the Kutta condition is satisfied, the dependence of the solution on a single parameter agrees with the present analysis. Their ω_2 free parameter results as $\omega_2 = -\log(R^2)/\pi$, and thus it is equivalent to the present choice of R as free parameter. Their normalization coincides with the present one.

https://doi.org/10.1017/S0022112010006154 Published online by Cambridge University Press

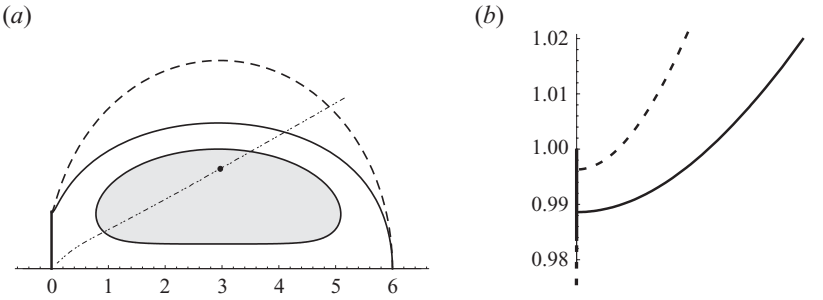


FIGURE 7. Hollow wake and point vortex wake for $R = 0.624$ and $z_B = 6.00$

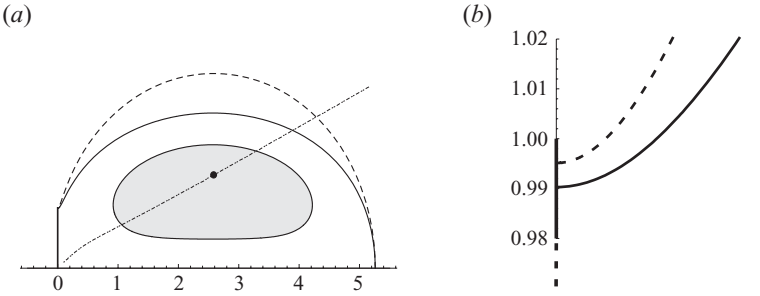


FIGURE 8. Hollow wake and point vortex wake for $R = 0.533$ and $z_B = 5.26$

They present three examples for R ($R_1 = 0.855$, $R_2 = 0.624$, $R_3 = 0.533$). The description of the results consists of just reporting the wake lengths and circulations, that is, the computed values of z_B ($z_{B_1} = 14.35$, $z_{B_2} = 6.00$, $z_{B_3} = 5.26$) and γ ($\gamma_1 = 24.42$, $\gamma_2 = 9.70$, $\gamma_3 = 8.19$).

Unfortunately, the paper of Lin & Landweber (1977) seems to have received very little consideration, and we have not been able to find other authors who have studied the same flow. In our opinion, their results deserve more attention; in fact, if correct, they show a continuation of hollow wakes which cannot end on a point vortex, since there is not a point vortex solution which satisfies the Kutta condition.

We have tried to use the present method to recompute the solutions of Lin & Landweber (1977), but enforcing the Kutta condition, our method did not converge for the above R_1, R_2 and R_3 values, nor for other smaller or greater values.

A different attempt to replicate their results has been made by enforcing the z_{B_1}, z_{B_2} and z_{B_3} computed locations of the reattachment points in a form mathematically equivalent to the Kutta condition. By so doing, the physical Kutta condition has been released. The results for (z_{B_2}, R_2) and (z_{B_3}, R_3) are shown in figures 7 and 8. They have been obtained by desingularizing the point vortices, with the same wake length, standing on the equilibrium locus (see Zannetti 2006). Figures 7(a) and 8(a) show the computed hollow wakes, the wakes pertinent to the point vortices (dotted line) and the point vortex equilibrium locus. Magnifications of the separatrices on the trailing edge region are shown in figures 7(b) and 8(b). These show that the hollow wakes violate the Kutta condition to a greater extent than the point vortex wakes.

The computed circulations are $\gamma_2 = -20.08$ and $\gamma_3 = -18.30$, which are close to the circulations $\gamma_{pv_2} = -22.06$ and $\gamma_{pv_3} = -19.42$ of the relevant point vortices and, apart

https://doi.org/10.1017/S0022112010006154 Published online by Cambridge University Press

from the opposite signs, are about twice as big as the values computed by Lin & Landweber (1977).

Our method was unable to converge to a solution for (z_{B_1}, R_1). This failure should be ascribed to the lack of robustness of the Garrick mapping for large values of R; solutions have in fact been obtained for z_{B_1} and for smaller values of R.

Unfortunately, Lin & Landweber (1977) did not provide their criterion of accuracy and convergence, so a doubt could arise concerning the correctness of their results. Nevertheless, the odd difference on the circulations of their and the present solutions could suggest, for a given (z_B, R), a multiplicity of solutions, which has not been detected by our computations.

5. Conclusions

It has been shown that point vortices standing in equilibrium in the flow past blunt obstacles can be desingularized by hollow vortices with growing cores.

In general, the solution depends on two free parameters which are related to the location of the separation/reattachment point and to the core geometry. When a Kutta condition is enforced, the number of the free parameters reduces to one.

A spectrally accurate mixed analytical numerical method has been developed, and numerical examples have been provided for growing hollow vortices in the wake past a semicircular obstacle and that past a Ringleb snow cornice.

The results of Lin & Landweber (1977) for the flow past a normal flat plate have been discussed and compared with the results obtained using the present method. The discrepancies between the two methods could suggest inaccuracy of the computations of Lin & Landweber (1977); nevertheless, the possibility of multiple solutions remains open.

REFERENCES

Batchelor, G. K. 1956 On steady laminar flows with closed streamlines at large Reynolds number. *J. Fluid Mech.* **1**, 177–190.

Birkoff, G. & Zarantonello, E. H. 1957 *Jets, Wakes, and Cavities*. Academic.

Chernyshenko, S. I. 1998 Asymptotic theory of global separation. *Appl. Mech. Rev.* **51**, 523–536.

Elcrat, A., Fornberg, B., Horn, M. & Miller, K. 2000 Some steady vortex flows past a circular cylinder. *J. Fluid Mech.* **409**, 13–27.

Gallizio, F. 2004 Modello di Prandtl–Batchelor per il flusso normale ad una placca piana posta all'interno di un canale: studio numerico dell'esistenza e unicità della soluzione. Dissertazione di Tesi Laurea, Ingegneria Aerospaziale, aa 2003/2004, Politecnico di Torino, Turin, Italy.

Gallizio, F., Iollo, A., Protas, B. & Zannetti, L. 2010 On continuation of inviscid vortex patches. *Physica* D **239**, 190–201.

Gilbarg, D. 1960 Jets and cavities. In *Handbuch der Physik* (ed. C. Truesdell), vol. 9, pp. 311–445. Springer.

Gurevich, M. I. 1965 *Theory of Jets in Ideal Fluids*. Academic.

Hicks, W. M. 1883 On the steady motion of a hollow vortex. *Proc. R. Soc. Lond.* **35**, 304–308.

Ives, D. C. 1976 A modern look at conformal mapping, including multiply connected regions. *AIAA J.* **14**, 1006–1011.

Lamb, H. 1932 *Hydrodynamics*. Cambridge University Press.

Lavrentiev, M. A. 1962 *Variational Methods for Boundary Value Problems for Systems of Elliptic Functions*. Noordhoff.

Levi-Civita, T. 1907 Scie e leggi di resistenza. *Rend. Circ. Mat. Palermo* **23**, 1–37.

Lin, A. & Landweber, L. 1977 On a solution of the Lavrentiev wake model and its cascade. *J. Fluid Mech.* **79**, 801–823.

https://doi.org/10.1017/S0022112010006154 Published online by Cambridge University Press

Nehari, Z. 1975 *Conformal Mapping*. Dover.

Pocklington, H. C. 1895 The configuration of a pair of equal and opposite hollow straight vortices, of finite cross-section, moving steadily through fluid. *Proc. Camb. Phil. Soc.* **8**, 178–187.

Ringleb, F. O. 1961 Separation control by trapped vortices. In *Boundary Layer and Flow Control* (ed. G. V. Lachman), pp. 265–294. Pergamon.

Smith, J. H. B. & Clark, R. W. 1986 Nonexistence of stationary vortices behind a two-dimensional normal plate. *AIAA J.* **13** (8), 1114–1115.

Tanveer, S. A. 1984 Topics in 2-D separated vortex flows. PhD thesis, California Institute of Technology.

Tanveer, S. A. 1986 A steadily translating pair of equal and opposite vortices with vortex sheets on their boundaries. *Stud. Appl. Maths* **74**, 139–154.

Tricomi, F. 1951 *Funzioni Ellittiche*. Zanichelli.

Turfus, C. 1993 Prandtl–Batchelor flow past a flat plate at normal incidence in a channel – inviscid analysis. *J. Fluid Mech.* **249**, 59–72.

Zannetti, L. 2006 Vortex equilibrium in the flow past bluff bodies. *J. Fluid Mech.* **562**, 151–171.

https://doi.org/10.1017/S0022112010006154 Published online by Cambridge University Press